

Comparing spatial and temporal transferability of hydrological model parameters

Patil, S.D.; Stieglitz, M.

Journal of Hydrology

DOI:
[10.1016/j.jhydrol.2015.04.003](https://doi.org/10.1016/j.jhydrol.2015.04.003)

Published: 09/04/2015

Peer reviewed version

[Cyswllt i'r cyhoeddiad / Link to publication](#)

Dyfyniad o'r fersiwn a gyhoeddwyd / Citation for published version (APA):
Patil, S. D., & Stieglitz, M. (2015). Comparing spatial and temporal transferability of hydrological model parameters. *Journal of Hydrology*, 525, 409-417.
<https://doi.org/10.1016/j.jhydrol.2015.04.003>

Hawliau Cyffredinol / General rights

Copyright and moral rights for the publications made accessible in the public portal are retained by the authors and/or other copyright owners and it is a condition of accessing publications that users recognise and abide by the legal requirements associated with these rights.

- Users may download and print one copy of any publication from the public portal for the purpose of private study or research.
- You may not further distribute the material or use it for any profit-making activity or commercial gain
- You may freely distribute the URL identifying the publication in the public portal ?

Take down policy

If you believe that this document breaches copyright please contact us providing details, and we will remove access to the work immediately and investigate your claim.

NOTICE: This is the author's version of a work that was peer reviewed and accepted for publication in the Journal of Hydrology. Changes resulting from the publishing process, such as editing, corrections, structural formatting, and other quality control mechanisms may not be reflected in this document. A definitive version was published in JOURNAL OF HYDROLOGY, VOL 525, DOI <http://dx.doi.org/10.1016/j.jhydrol.2015.04.003>.

Comparing spatial and temporal transferability of hydrological model parameters

Sopan D. Patil¹, Marc Stieglitz²

¹ School of Environment, Natural Resources and Geography,
Bangor University,
Deiniol Road, Bangor, LL57 2UW, United Kingdom

² School of Civil and Environmental Engineering,
Georgia Institute of Technology,
790 Atlantic Drive, Atlanta, GA 30332, United States of America

Submission to: Journal of Hydrology

Correspondence to: Sopan D. Patil (email: s.d.patil@bangor.ac.uk, Tel: +44 1248 388294)

Highlights:

- 1) We compare three different schemes for transfer of hydrological model parameters
- 2) Temporal transfer scheme outperforms spatial and spatiotemporal transfer schemes
- 3) Differences between spatial and spatiotemporal transfer schemes are negligible
- 4) Temporal gap in calibration and validation periods reduces difference among schemes

Abstract

Operational use of hydrological models requires the transfer of calibrated parameters either in time (for streamflow forecasting) or space (for prediction at ungauged catchments) or both. Although the effects of spatial and temporal parameter transfer on catchment streamflow predictions have been well studied individually, a direct comparison of these approaches is much less documented. Here, we compare three different schemes of parameter transfer, viz., temporal, spatial, and spatiotemporal, using a spatially lumped hydrological model called EXP-HYDRO at 294 catchments across the continental United States. Results show that the temporal parameter transfer scheme performs best, with lowest decline in prediction performance (median decline of 4.2%) as measured using the Kling-Gupta efficiency metric. More interestingly, negligible difference in prediction performance is observed between the spatial and spatiotemporal parameter transfer schemes (median decline of 12.4% and 13.9% respectively). We further demonstrate that the superiority of temporal parameter transfer scheme is preserved even when: (1) spatial distance between donor and receiver catchments is reduced, or (2) temporal lag between calibration and validation periods is increased. Nonetheless, increase in the temporal lag between calibration and validation periods reduces the overall performance gap between the three parameter transfer schemes. Results suggest that spatiotemporal transfer of hydrological model parameters has the potential to be a viable option for climate change related hydrological studies, as envisioned in the “trading space for time” framework. However, further research is still needed to explore the relationship between spatial and temporal aspects of catchment hydrological variability.

Keywords: Hydrological model; parameter transfer; catchment; streamflow prediction

1 Introduction

All hydrological models contain parameters whose values must be calibrated by comparing the observed and simulated streamflow values from the past record [Refsgaard, 1997; Beven, 2001]. Calibrated parameters represent the unique combination of climatic and physiographic factors that influence the hydrological behaviour of a catchment [Merz and Blöschl, 2004; Wagener and Wheeler, 2006]. However, operational use of hydrological models is always outside of the calibration period and/or catchment, which is where the parameters face their true test [Klemeš, 1986; Refsgaard and Knudsen, 1996; Coron et al., 2012]. Parameter transfer away from this calibration domain can be in time (for streamflow forecasting) or space (for prediction at ungauged catchments) or both.

Temporal transfer of calibrated parameters is perhaps the most common and straightforward procedure used in catchment hydrological modelling. The first step involves choosing a specific historical time period for which all the input and output data required for running the model are available for the catchment. These data are used to calibrate the model parameters by finding the best match between the simulated and observed streamflow values. This procedure is followed by the application of the calibrated model at some other time period in the same catchment. Klemeš [1986] recommends that testing of hydrological models outside the calibration period is critical to establish their credibility as useful forecasting tools. An implicit assumption here is that the calibrated model parameters are temporally stable, i.e., they are suitable for application beyond the calibration period. However, numerous recent studies have shown that hydrological model parameters are not always temporally stable [Merz et al., 2011; Brigode et al., 2013; Westra et al., 2014], and their values depend on the duration as well as the specific physioclimatic conditions of the calibration period [Xia et al., 2004; Juston et al., 2009; Vaze et al., 2010; Razavi and Tolson, 2013]. Wagener et al. [2003] used dynamic identifiability analysis (DYNIA) to estimate the

parameters of a spatially lumped hydrological model and found that parameter values varied significantly when calibrated to different parts of the hydrograph. *Merz et al.* [2011] calibrated the parameters of a semi-distributed version of HBV model for six consecutive 5 year periods between 1976 and 2006 at 273 Austrian catchments, and found that (1) optimal parameter values were variable across the six calibration periods, and (2) the assumption of time invariant parameters had a significant impact on model simulations outside the calibration period. Similar findings were reported by *Coron et al.* [2012] in their study on temporal parameter transfer using three rainfall-runoff models at 216 catchments in southeast Australia. *Razavi and Tolson* [2013] compared three different calibration approaches for the SWAT2000 model at a catchment in the state of New York, USA and concluded that “...model calibration solely to a short data period may lead to a range of performances from poor to very well depending on the representativeness of the short data period which is typically not known a priori”.

Spatial transfer of calibrated parameters is another widely used procedure in catchment hydrological modelling and is primarily required for streamflow prediction at ungauged basins (PUB) [*Sivapalan et al.*, 2003]. A considerable amount of research has been conducted over the years in the development and comparison of approaches to transfer hydrological model parameters from gauged to ungauged catchments [*Post and Jakeman*, 1999; *Kokkonen et al.*, 2003; *McIntyre et al.*, 2005; *Young*, 2006; *Oudin et al.*, 2008; *Zhang and Chiew*, 2009; *Patil and Stieglitz*, 2014]. *Blöschl et al.* [2013] and *Hrachowitz et al.* [2013] provide a comprehensive summary and synthesis of the progress made in PUB research during the International Association of Hydrological Sciences’ (IAHS) PUB decade initiative (2003-2012) [*Sivapalan et al.*, 2003]. Donor gauged catchments, from which model parameters can be transferred to the receiver ungauged catchments, are typically identified using an approach that is either based on spatial proximity or physical similarity to the

74 ungauged catchments. *Oudin et al.* [2008] compared the spatial proximity and physical
75 similarity approaches at 913 catchments in France and found that the spatial proximity
76 approach outperformed the physical similarity approach. *Zhang and Chiew* [2009] tested
77 multiple parameter transfer approaches at 210 catchments in southeast Australia and found
78 that an integrated similarity approach that combined spatial proximity and physical similarity
79 slightly outperformed the spatial proximity approach. *Patil and Stieglitz* [2014] compared
80 two different methods of spatial parameter transfer at 323 catchments in the United States and
81 found that simulation performance at ungauged catchments is more sensitive to the types of
82 parameters that are transferred than to the method used for transferring them. However,
83 regardless of the chosen approach, spatial parameter transfer tends to cause deterioration in
84 simulation performance (compared to calibration) due to the differences in physiographic
85 properties and meteorological inputs between the donor and receiver catchments.

86 Although hydrological model simulation following temporal and/or spatial parameter
87 transfer is expected to cause deterioration in catchment streamflow prediction, not many
88 studies have focused on a direct comparison of these two approaches. A few PUB focused
89 studies that have made such a comparison show results that range from a large performance
90 difference between temporal and spatial parameter transfer (in favour of temporal) [*Merz and*
91 *Blöschl*, 2004; *Parajka et al.*, 2005] to minor performance difference between them [*Oudin et*
92 *al.*, 2008]. In our view, further exploration is therefore needed on how the spatial and
93 temporal parameter transfer approaches compare against each other, especially in the context
94 of increasing appeal and popularity of the “trading space for time” approaches that are
95 proposed for assessing the hydrological implications of anthropogenic climate change
96 [*Wagener et al.*, 2010; *Peel and Blöschl*, 2011; *Singh et al.*, 2011; *Ehret et al.*, 2014;
97 *Refsgaard et al.*, 2014]. The trading space for time framework assumes that the spatial
98 variability in catchment hydrological properties (including model parameters) can be used as

a proxy for the climate change induced temporal variability in those properties [Merz *et al.*, 2011]. Studies such as Singh *et al.* [2011, 2014] have already demonstrated that the spatial parameter regionalization techniques developed for PUB can also be applied to make temporal modifications in model parameters for streamflow predictions under change (PUC) [Montanari *et al.*, 2013]. Therefore, we argue that a systematic comparison of the spatial and temporal parameter transfer approaches is likely to provide further insights into the connections between the PUB and PUC paradigms, and could even help refine the trading space for time methods.

In this paper, we compare three schemes of model parameter transfer, viz., temporal, spatial, and spatiotemporal, using a hydrological model called EXP-HYDRO [Patil and Stieglitz, 2014; Patil *et al.*, 2014a, 2014b] at 294 catchments across the continental United States. The temporal parameter transfer scheme is implemented using a split-sample test procedure where the available data is divided into two periods, one for calibration and the other for validation. For the spatial parameter transfer scheme, we use the nearest neighbour catchment as a donor of calibrated parameters. Comparison of different spatial parameter transfer techniques is beyond the scope of this study (and has already been done by Patil and Stieglitz [2014]). In the spatiotemporal parameter transfer scheme, calibrated model parameters are transferred simultaneously in the spatial (to the nearest neighbour catchment) and temporal (to a different time period) domain.

2 Data and Methods

2.1 Hydrological Model

We use the spatially lumped version of EXP-HYDRO model [Patil and Stieglitz, 2014; Patil *et al.*, 2014a, 2014b] to simulate daily streamflow (Figure 1). This model solves the following two coupled ordinary differential equations simultaneously at each time step:

$$\frac{dS_{Snow}}{dt} = P_{Snow} - Q_{Melt} \quad (1a)$$

$$\frac{dS}{dt} = P_{Rain} + Q_{Melt} - ET - Q_{Bucket} - Q_{Spill} \quad (1b)$$

where S and S_{Snow} are, respectively, the amounts of stored water (mm) in the catchment and snow accumulation buckets. P_{Snow} and P_{Rain} are the snowfall and rainfall amounts (mm/day). ET is the actual evapotranspiration (mm/day) from the catchment bucket. Q_{Melt} is the snowmelt (mm/day) from the snow accumulation bucket, Q_{Bucket} is the subsurface runoff (mm/day) generated from the catchment bucket, and Q_{Spill} is the capacity-excess surface runoff (mm/day) that is generated when the catchment bucket is filled to capacity.

The incoming daily precipitation P is classified as snowfall or rainfall based on the following conditions:

If $T_a < T_{min}$,

$$\begin{aligned} P_{Snow} &= P \\ P_{Rain} &= 0 \end{aligned} \quad (2a)$$

Else,

$$\begin{aligned} P_{Snow} &= 0 \\ P_{Rain} &= P \end{aligned} \quad (2b)$$

where T_a is the actual air temperature on a given day, T_{min} is the air temperature below which the precipitation occurs as snowfall and falls directly into the snow accumulation bucket.

Snowmelt Q_{Melt} is modelled using a simple thermal degree day model as follows:

If $T_a > T_{max}$,

$$Q_{Melt} = \min \{ S_{Snow}, D_f \cdot (T_a - T_{max}) \} \quad (3a)$$

Else,

$$Q_{Melt} = 0 \quad (3b)$$

where T_{max} is the air temperature above which the snow in snow accumulation bucket starts melting, and D_f is the thermal degree day factor that controls the rate of snowmelt.

Evapotranspiration ET from the catchment bucket is calculated as follows:

$$ET = PET \cdot \left(\frac{S}{S_{max}} \right) \quad (4)$$

where PET is the potential evapotranspiration (mm/day), and is calculated from the daily air temperature using Hamon's formula [Hamon, 1963]. S_{max} is the total storage capacity (mm) of the catchment bucket. The surface and subsurface runoff generated from the catchment bucket are calculated as follows:

If $S \leq S_{max}$,

$$\begin{aligned} Q_{Bucket} &= Q_{max} \cdot \exp(-f \cdot (S_{max} - S)) \\ Q_{Spill} &= 0 \end{aligned} \quad (5a)$$

If $S > S_{max}$,

$$\begin{aligned} Q_{Bucket} &= Q_{max} \\ Q_{Spill} &= S - S_{max} \end{aligned} \quad (5b)$$

where Q_{max} is the maximum subsurface runoff produced (mm/day) when the catchment bucket reaches its capacity, and f is the parameter controlling the storage-dependent exponential decline in subsurface runoff (1/mm). Daily streamflow at the catchment outlet is the sum of Q_{Bucket} and Q_{Spill} .

We have now made the entire source code of the spatially lumped version of the EXP-HYDRO model (described above) freely available to the research community. This source code is written in Python ® programming language and can be downloaded from the following web link: <http://sopanpatil.weebly.com/exp-hydro.html>.

2.2 Model Calibration

There are six calibration parameters in the EXP-HYDRO model: f , S_{\max} , Q_{\max} , D_f , T_{\max} , and T_{\min} . For each catchment, we calibrate these six model parameters using the Particle Swarm Optimisation (PSO) algorithm [Kennedy and Eberhart, 1995]. PSO is a stochastic population-based search algorithm that has been used in numerous hydrological studies for model parameter calibration [Gill *et al.*, 2006; Goswami and O'Connor, 2007; Liu, 2009; Zhang *et al.*, 2009]. PSO is initialised with a group of random particles (parameter sets in our case), and this ‘swarm’ of particles searches for an optimal solution within the parameter domain by iteratively updating the velocity and position of each particle. We initialise the PSO algorithm with 10 randomly generated EXP-HYDRO parameter sets (sampled from a uniform distribution) and allow for a maximum of 50 swarm iterations to find the optimal solution. The upper and lower bound values of all six parameters are same as those in Patil and Stieglitz [2014]. We use Kling-Gupta efficiency (KGE) [Gupta *et al.*, 2009] as the objective function that is to be maximised during calibration:

$$KGE = 1 - \sqrt{(r-1)^2 + (\alpha-1)^2 + (\beta-1)^2} \quad (6)$$

where r is the Pearson’s linear correlation coefficient between the observed and simulated streamflow, α is the ratio of standard deviations of observed and simulated streamflow, and β is the ratio of mean values of observed and simulated streamflow. The value of KGE varies from $-\infty$ to 1, with $KGE = 1$ being a perfect fit between the observed and simulated values.

As shown by Gupta *et al.* [2009], KGE consists of three main components, correlation (g_1), variability (g_2), and bias (g_3), whose relative contribution to the KGE value varies from 0 to 1 and is calculated as follows:

$$g_i = \frac{G_i}{\sum_{j=1}^3 G_j} \quad (7a)$$

and,

$$\begin{aligned} G_1 &= (r-1)^2 \\ G_2 &= (\alpha-1)^2 \\ G_3 &= (\beta-1)^2 \end{aligned} \quad (7b)$$

2.3 Study Catchments

We begin the catchment selection process by implementing the EXP-HYDRO model at 756 catchments in the continental United States (Figure 2a). These are the same catchments that have been used in our two previous studies [Patil and Stieglitz, 2012, 2014]; they belong to the U. S. Geological Survey's Hydro-Climate Data Network (HCDN) [Slack et al., 1993] and have a continuous daily streamflow record from water year (WY) 1970 to 1988 (i.e., 1st October, 1969 to 30th September, 1988). Daily precipitation and air temperature data for each catchment are obtained from the gridded meteorological dataset developed by Maurer et al. [2002]. This data has a spatial resolution of 0.125 degree and covers the entire continental United States.

We split the timeline from WY 1970 to 1988 into the following three periods: WY 1970 is the spin-up period that is not used for parameter calibration, WY 1971 to 1978 is calibration period 1, and WY 1979 to 1988 is calibration period 2 (see Figure 2b). For each catchment, we calibrate the EXP-HYDRO model parameters separately for calibration periods 1 and 2 using the methods described in Section 2.2. Only those catchments where the simulated streamflow provides $KGE > 0.6$ for both calibration periods are retained as our study catchments. This is done to ensure that only those catchments for which the EXP-HYDRO model structure seems suitable for providing good hydrological simulations are used for any further analyses. The above condition reduces the number of acceptable study

catchments to 294 (Figure 2a). The geographic distribution of the acceptable catchments is similar to that obtained by *Patil and Stieglitz* [2014]. The drainage area of the study catchments ranges from 24 km² to 4790 km², with median drainage area of 620 km². The majority of catchments are located in the eastern part of the continental United States, to the east of Mississippi River. In the western United States, the study catchments are primarily located along the Rocky, Cascade and Pacific Coastal mountain ranges. Mean annual precipitation among the study catchments ranges from 340 mm to 2556 mm (median = 1160 mm).

2.4 Parameter Transfer Schemes

For the 294 study catchments, we test the following three schemes of model parameter transfer:

- (1) Temporal transfer: For the same catchment, model parameters from calibration period 1 are transferred to calibration period 2, and vice versa.
- (2) Spatial transfer: Model parameters of a catchment are obtained from its nearest neighbour catchment over the same time period. This is done separately for calibration periods 1 and 2.
- (3) Spatiotemporal transfer: Model parameters of a catchment are obtained from its nearest neighbour catchment across different time periods (i.e., from calibration period 1 to 2, and vice versa).

3 Results

We first compare the simulation performance of EXP-HYDRO model that is obtained across the two calibration periods. Figure 3 shows a 1:1 comparison of the KGE values obtained at the 294 catchments during calibration periods 1 and 2. The relationship between calibrated KGE values of the two periods is somewhat weak (Pearson's $r = 0.53$), with data

points scattered along both sides of the 1:1 line. Figure 4 shows the comparison of g_1 , g_2 , and g_3 (the three components of KGE) during calibration periods 1 and 2. Similar to KGE, a weak relationship exists between the values obtained at these two different periods ($r = 0.55$ for g_1 , $r = 0.4$ for g_2 , $r = 0.65$ for g_3). Figures 5a-f show a 1:1 comparison of the values of all six EXP-HYDRO parameters during calibration periods 1 and 2. The relationship among parameter values across the two calibration periods is strongest for f ($r = 0.81$, Figure 5a), followed by S_{\max} ($r = 0.59$, Figure 5b), D_f ($r = 0.36$, Figure 5d), Q_{\max} ($r = 0.26$, Figure 5c), T_{\min} ($r = 0.26$, Figure 5e), and T_{\max} ($r = 0.17$, Figure 5f).

We next compare the performance of EXP-HYDRO model across the three parameter transfer schemes. Figure 6 shows a box-plot comparison of the KGE values among the following four modelling scenarios: calibration, temporal transfer, spatial transfer, and spatiotemporal transfer. Note that the KGE values shown in Figure 6 are the average values of two sub-scenarios that are present in each scenario. For example, KGE of each catchment in the calibration scenario is an average of its KGE values from calibration period 1 and calibration period 2. As seen in Figure 6, the overall model performance is highest for the calibration scenario (median KGE = 0.72), followed by temporal transfer (median KGE = 0.69; decline of 4.2% (compared to calibration)), spatial transfer (median KGE = 0.63; decline of 12.4%), and spatiotemporal transfer (median KGE = 0.62; decline of 13.9%) scenarios.

Figure 7 shows the box-plot comparison of the above four scenarios with respect to the three KGE components, g_1 , g_2 , and g_3 . For correlation component g_1 , calibration scenario has the highest overall contribution value (median $g_1 = 0.85$), and is followed by temporal (median $g_1 = 0.68$), spatial (median $g_1 = 0.54$), and spatiotemporal (median $g_1 =$

0.54) transfer scenarios. For variability component g_2 , calibration scenario has the lowest contribution value (median $g_2 = 0.06$), and is followed by the temporal (median $g_2 = 0.17$), spatial (median $g_2 = 0.23$), and spatiotemporal (median $g_2 = 0.24$) transfer schemes. The bias component g_3 has a similar trend as g_2 , but is less prominent. The calibration scenario has the lowest contribution value (median $g_3 = 0.05$), and is followed by the temporal (median $g_3 = 0.11$), spatial (median $g_3 = 0.12$), and spatiotemporal (median $g_3 = 0.13$) transfer schemes.

Results from Figures 6 and 7 demonstrate that the overall model performance of the temporal parameter transfer scheme is superior to that of the spatial and spatiotemporal parameter transfer schemes. However, it is not clear from these results whether our experimental setup provides any undue advantage to the temporal parameter transfer scheme over the other two schemes. Below, we briefly mention two such potential scenarios:

Scenario 1: It is likely that for some of our study catchments, the distance between them and their nearest neighbour catchment is too high. Such a scenario puts the spatial and spatiotemporal transfer schemes at a clear disadvantage compared to the temporal transfer scheme.

Scenario 2: There is no temporal lag between calibration periods 1 and 2, i.e., calibration period 2 immediately follows calibration period 1 (Figure 2b). For catchments where the meteorological input patterns have not changed much across the two periods, the temporal parameter transfer scheme is much more likely to outperform the other two schemes.

To mitigate the impacts from above two potential scenarios on our results, we repeat the parameter transfer experiment for the two following special conditions:

Special Condition 1: Eliminate all study catchments that have a nearest neighbour catchment more than 50 km away. The 50 km distance limit is slightly less than the median nearest

neighbour distance (53.1 km) among all the 294 study catchments. This reduces the number of catchments from 294 to 138.

Special Condition 2: Shorten the calibration period 1 to span from WY 1971 to 1975 (instead of WY 1971 to 1978) and calibration period 2 to span from WY 1984 to 1988 (instead of WY 1979 to 1988). This creates a temporal lag of 8 years between the two calibration periods. Nonetheless, unlike Special Condition 1, all 294 study catchments are used for simulations. Note that these new calibration periods span 5 years each, which is the minimum time span recommended by some studies to adequately capture the temporal hydrological variability of a catchment [Merz *et al.*, 2009].

Figures 8a and 8b show the box-plot comparison of KGE values from the four modelling scenarios for Special Conditions 1 and 2 respectively. In both cases, the results are similar to those observed in Figure 6. For Special Condition 1, the highest model performance is obtained for the calibration scenario (median KGE = 0.74), followed by the temporal (median KGE = 0.71; decline of 4%), spatial (median KGE = 0.67; decline of 9.5%), and spatiotemporal (median KGE = 0.66; decline of 10.8%) parameter transfer schemes. For Special Condition 2, the median KGE values are 0.72 for calibration, 0.66 for temporal transfer scheme (decline of 8.3%), 0.62 for spatial transfer scheme (decline of 13.9%), and 0.62 for spatiotemporal transfer scheme (decline of 13.9%).

4 Discussion

Comparison of the optimal KGE values (Figure 3) and the individual KGE components (Figure 4) between calibration periods 1 and 2 demonstrates that the performance of a hydrological model can, at least in some cases, vary considerably in the same catchment for different calibration periods. Similar findings have been reported by Vaze *et al.* [2010] and Razavi and Tolson [2013]. The data points shown in Figures 3 and 4

are scattered along both sides of the 1:1 line. This suggests that for our study catchments no systematic bias exists in terms of one calibration period providing better calibration performance than the other. For the majority of study catchments (213 out of 294), the difference between optimal KGE values for the two calibration periods is less than 10% (median = 6%). This is consistent with *Merz et al.* [2011], who found that the calibrated Nash-Sutcliffe efficiency values [*Nash and Sutcliffe*, 1970] of the HBV model, averaged across their 273 Austrian catchments, showed small variability across six different calibration periods. However, they found this variability to increase when only drier study catchments were considered in their calculations. Although our data set does have a few catchments that show large performance difference between the calibration periods (largest difference is 35%), we did not detect any specific geographic or climatic pattern among those catchments.

Results from Figure 5 show that the temporal variability of parameter values is different for each parameter, with values of the f parameter showing the highest correlation (and therefore lowest variability) between the two calibration periods, followed by S_{\max} , D_f , Q_{\max} , T_{\min} , and T_{\max} . Interestingly, this trend is similar to the parameter sensitivity trend shown in our previous study [*Patil and Stieglitz*, 2014]. *Patil and Stieglitz* [2014] performed a sensitivity analysis of all 6 EXP-HYDRO parameters and found that f , S_{\max} , and D_f were the most sensitive parameters (i.e., sensitive to the objective function) with better defined optimal values and posterior distributions. On the other hand, Q_{\max} , T_{\min} , and T_{\max} were characterised as the insensitive parameters with virtually no difference between their prior (uniform) and posterior distributions. Combined, these results suggest that the high sensitivity model parameters are also more likely to have low variability across different calibration periods, thereby making them more representative of the catchment's intrinsic physiographic conditions rather than the specific input conditions during the calibration

period. For the EXP-HYDRO model, the two most temporally stable parameters (f and S_{\max}) represent: (1) the rate of storage decline within the soil bucket in response to subsurface runoff, and (2) the total soil bucket capacity. Both these parameters are, at least in theory, linked to the intrinsic soil and topographic properties of a catchment that are unlikely to undergo drastic temporal change. Nonetheless, we suspect that the proportion of sensitive and temporally stable parameters is likely to be different for different types of hydrological models. For instance, *Merz and Blöschl* [2004] calibrated the lumped version of HBV model (containing 11 parameters) at 308 catchments in Austria for two different calibration periods. They found that the correlation coefficient (R^2) between the parameter values of the two calibration periods ranged from 0.09 to 0.64, with only 5 of the 11 parameters having $R^2 > 0.5$. *Oudin et al.* [2008] compared the parameters of two spatially lumped hydrological models, GR4J (4 parameters) and TOPMO (6 parameters), for 913 French catchments across two calibration periods, and showed that the correlation across calibration periods was higher for GR4J parameters compared to TOPMO parameters. However, it must be noted we still do not have a complete understanding of how these model parameter values will change in response to land cover changes within a catchment [*Eckhardt et al.*, 2003; *Croke et al.*, 2004; *Wang and Kalin*, 2011].

Results from the parameter transfer experiment (Figures 6 and 7) demonstrate the overall superior performance of the temporal parameter transfer scheme over the spatial and spatiotemporal parameter transfer schemes. Analysis of the three KGE components (Figure 7) shows that the correlation component (g_1) is the most dominant contributor to KGE value, which is consistent with *Gupta et al.* [2009]. However, this component also undergoes the most decline when moving away from calibration to the parameter transfer scenarios. The decline in g_1 is compensated by a proportional increase in the contribution from the other two

components (variability g_2 and bias g_3) for the parameter transfer scenarios compared to calibration. *Gupta et al.* [2009] note that the relative contributions of the bias and variability components tend to increase for non-optimal parameter sets, as is observed in all our parameter transfer scenarios. When the three parameter transfer schemes are individually compared across each of the 294 catchments, the temporal transfer scheme shows best performance at 204 catchments (and worst at 50 catchments), the spatial transfer scheme is best at 65 catchments (and worst at 106 catchments), whereas the spatiotemporal transfer scheme is best at 27 catchments (and worst at 147 catchments). Figure 9 shows the map of catchment locations where either the spatial or spatiotemporal parameter transfer scheme is the best performing scheme. No specific geographic pattern is noticeable from this figure in terms of the catchments that prefer the spatial and spatiotemporal transfer schemes over the temporal transfer scheme. Table 1 shows the comparison of these two catchment groups (Group 1: spatial or spatiotemporal transfer scheme performing best; Group 2: temporal transfer scheme performing best) with respect to three commonly used hydro-climatic metrics, viz., mean annual rainfall (P), annual runoff ratio (Q/P) and climate aridity index (PET/P). Although the median values of these metrics suggest that Group 1 catchments are slightly drier (lower P and higher PET/P) and flashier (higher Q/P), there does not seem to be much difference among the two catchment groups. Nonetheless, Figure 9 clearly illustrates that even in regions with low catchment density and larger distances among neighbouring catchments (e.g., in the western US), the temporal parameter transfer schemes does not always outperform the spatial and spatiotemporal schemes.

Parameter transfer experiments under the two special conditions (see Section 3) show that the temporal parameter transfer scheme still preserves its advantage over the spatial and spatiotemporal schemes. For Special Condition 1, i.e., when only those catchments with nearest neighbour < 50 km away are retained, the spatial and spatiotemporal schemes exhibit

performance improvement as the KGE difference between them and calibration is about 3% lower than the base scenario. This is an expected result because lower spatial distances between catchments will most likely reduce the spatial variability of hydrological behaviour [Oudin *et al.*, 2008]. On the other hand, for Special Condition 2 (when the temporal gap between calibration periods is increased to 8 years), the KGE difference between calibration and the temporal scheme is about 4% higher than the base scenario, and is virtually unchanged between calibration and the spatial and spatiotemporal schemes. Thus, an increase in the temporal distance between calibration and validation periods reduces the model performance gap between the temporal scheme and the spatial and spatiotemporal schemes. This has important implications for the “trading space for time” framework [Peel and Blöschl, 2011; Refsgaard *et al.*, 2014] because a sufficiently large time lag between the calibration and validation periods (as is common in climate change scenarios) has the potential to make spatiotemporal parameter transfer a more viable option than temporal parameter transfer. However, even though the introduction of an 8 year temporal gap between the calibration and validation periods shows reduced performance gap among the parameter transfer schemes, it is not entirely clear how these schemes will compare for much larger (> 40-50 years) temporal gaps.

5 Conclusion

In this paper, we compared three different schemes for the transfer of hydrological model parameters, viz., temporal, spatial, and spatiotemporal, using a spatially lumped hydrological model called EXP-HYDRO at 294 catchments across the continental United States. In our view, such a comparison is highly relevant especially within the context of increasing appeal and popularity of the “trading space for time” framework proposed for assessing the hydrological implications of anthropogenic climate change. Results showed

that the temporal parameter transfer scheme performs best, with lowest decline in prediction performance compared to calibration (median decline of 4.2%); whereas negligible difference in prediction performance was observed between the spatial and spatiotemporal parameter transfer schemes (median decline of 12.4% and 13.9% respectively). These results suggest that the stability of hydrological model parameters tends to be higher in the temporal domain than in the spatial domain, and are consistent with previous studies conducted in different parts of the world [Parajka *et al.*, 2005; Zhang and Chiew, 2009]. We also demonstrated that the relative superiority of temporal parameter transfer scheme is preserved even when: (1) the spatial distance between donor and receiver catchments is reduced, or (2) the temporal lag between calibration and validation periods is increased. Nonetheless, we found that an increase in the temporal lag between calibration and validation periods reduces the model performance gap between the temporal scheme and the spatial and spatiotemporal schemes. This finding, combined with the negligible difference observed between the spatial and spatiotemporal schemes, suggest that spatiotemporal transfer of hydrological model parameters has the potential to be a viable option for climate change related studies, as envisioned in the trading space for time framework. However, further research is still needed to better understand the relationship between the spatial and temporal aspects of catchment hydrological variability with increasing time lag between the calibration and validation periods.

Acknowledgements

We are thankful to Mark Rayment and an anonymous reviewer for providing valuable comments and suggestions that have greatly improved this paper. This research was supported in part by the US National Science Foundation (NSF) grants 0922100 and

1027870. Mention of trade names or commercial products does not constitute endorsement
or recommendation for use.

References

- Beven, K. J. (2001), *Rainfall-runoff modelling: the primer*, Wiley, Chichester.
- Blöschl, G., M. Sivapalan, and T. Wagener (2013), *Runoff prediction in ungauged basins: synthesis across processes, places and scales*, Cambridge University Press.
- Brigode, P., L. Oudin, and C. Perrin (2013), Hydrological model parameter instability: A source of additional uncertainty in estimating the hydrological impacts of climate change?, *J. Hydrol.*, 476, 410–425, doi:10.1016/j.jhydrol.2012.11.012.
- Coron, L., V. Andréassian, C. Perrin, J. Lerat, J. Vaze, M. Bourqui, and F. Hendrickx (2012), Crash testing hydrological models in contrasted climate conditions: An experiment on 216 Australian catchments, *Water Resour. Res.*, 48(5), W05552, doi:10.1029/2011WR011721.
- Croke, B. F. W., W. S. Merritt, and A. J. Jakeman (2004), A dynamic model for predicting hydrologic response to land cover changes in gauged and ungauged catchments, *J. Hydrol.*, 291(1–2), 115–131, doi:http://dx.doi.org/10.1016/j.jhydrol.2003.12.012.
- Eckhardt, K., L. Breuer, and H. G. Frede (2003), Parameter uncertainty and the significance of simulated land use change effects, *J. Hydrol.*, 273(1–4), 164–176, doi:10.1016/S0022-1694(02)00395-5.
- Ehret, U. et al. (2014), Advancing catchment hydrology to deal with predictions under change, *Hydrol. Earth Syst. Sci.*, 18(2), 649–671, doi:10.5194/hess-18-649-2014.
- Gill, M. K., Y. H. Kaheil, A. Khalil, M. McKee, and L. Bastidas (2006), Multiobjective particle swarm optimization for parameter estimation in hydrology, *Water Resour. Res.*, 42(7), W07417, doi:10.1029/2005WR004528.
- Goswami, M., and K. M. O'Connor (2007), Comparative assessment of six automatic optimization techniques for calibration of a conceptual rainfall—runoff model, *Hydrol. Sci. J.*, 52(3), 432–449, doi:10.1623/hysj.52.3.432.
- Gupta, H. V., H. Kling, K. K. Yilmaz, and G. F. Martinez (2009), Decomposition of the mean squared error and NSE performance criteria: Implications for improving hydrological modelling, *J. Hydrol.*, 377(1–2), 80–91, doi:10.1016/j.jhydrol.2009.08.003.
- Hamon, W. R. (1963), Computation of direct runoff amounts from storm rainfall, *Int. Assoc. Sci. Hydrol. Publ*, 63, 52–62.

462 Hrachowitz, M. et al. (2013), A decade of Predictions in Ungauged Basins (PUB)—a review,
 463 *Hydrol. Sci. J.*, 58(6), 1198–1255, doi:10.1080/02626667.2013.803183.

464 Juston, J., J. Seibert, and P.-O. Johansson (2009), Temporal sampling strategies and
 465 uncertainty in calibrating a conceptual hydrological model for a small boreal catchment,
 466 *Hydrol. Process.*, 23(21), 3093–3109, doi:10.1002/hyp.7421.

467 Kennedy, J., and R. Eberhart (1995), Particle swarm optimization, in *IEEE International*
 468 *Conference on Neural Networks Proceedings, Vols 1-6*, pp. 1942–1948.

469 Klemeš, V. (1986), Operational testing of hydrological simulation models, *Hydrol. Sci. J.*,
 470 31(1), 13–24, doi:10.1080/02626668609491024.

471 Kokkonen, T. S., A. J. Jakeman, P. C. Young, and H. J. Koivusalo (2003), Predicting daily
 472 flows in ungauged catchments: model regionalization from catchment descriptors at the
 473 Coweeta Hydrologic Laboratory, North Carolina, *Hydrol. Process.*, 17, 2219–2238,
 474 doi:10.1002/hyp.1329.

475 Liu, Y. (2009), Automatic calibration of a rainfall–runoff model using a fast and elitist multi-
 476 objective particle swarm algorithm, *Expert Syst. Appl.*, 36(5), 9533–9538,
 477 doi:10.1016/j.eswa.2008.10.086.

478 Maurer, E. P., A. W. Wood, J. C. Adam, D. P. Lettenmaier, and B. Nijssen (2002), A Long-
 479 Term Hydrologically Based Dataset of Land Surface Fluxes and States for the
 480 Conterminous United States, *J. Clim.*, 15, 3237–3251, doi:10.1175/1520-
 481 0442(2002)015<3237:althbd>2.0.co;2.

482 McIntyre, N., H. Lee, H. Wheater, A. Young, and T. Wagener (2005), Ensemble predictions
 483 of runoff in ungauged catchments, *Water Resour. Res.*, 41, W12434,
 484 doi:10.1029/2005wr004289.

485 Merz, R., and G. Blöschl (2004), Regionalisation of catchment model parameters, *J. Hydrol.*,
 486 287(1-4), 95–123, doi:10.1016/j.jhydrol.2003.09.028.

487 Merz, R., J. Parajka, and G. Blöschl (2009), Scale effects in conceptual hydrological
 488 modeling, *Water Resour. Res.*, 45(9), W09405, doi:10.1029/2009WR007872.

489 Merz, R., J. Parajka, and G. Blöschl (2011), Time stability of catchment model parameters:
 490 Implications for climate impact analyses, *Water Resour. Res.*, 47(2), W02531,
 491 doi:10.1029/2010WR009505.

492 Montanari, A. et al. (2013), “Panta Rhei—Everything Flows”: Change in hydrology and
 493 society—The IAHS Scientific Decade 2013–2022, *Hydrol. Sci. J.*, 58(6), 1256–1275,
 494 doi:10.1080/02626667.2013.809088.

495 Nash, J. E., and J. V Sutcliffe (1970), River flow forecasting through conceptual models part
 496 I — A discussion of principles, *J. Hydrol.*, 10, 282–290, doi:10.1016/0022-
 497 1694(70)90255-6.

498 Oudin, L., V. Andreassian, C. Perrin, C. Michel, and N. Le Moine (2008), Spatial proximity,
 499 physical similarity, regression and ungauged catchments: A comparison of regionalization
 500 approaches based on 913 French catchments, *Water Resour. Res.*, 44(3), W03413–
 501 W03413, doi:10.1029/2007WR006240.

502 Parajka, J., R. Merz, and G. Blöschl (2005), A comparison of regionalisation methods for
 503 catchment model parameters, *Hydrol. Earth Syst. Sci.*, 9(3), 157–171.

504 Patil, S., and M. Stieglitz (2012), Controls on hydrologic similarity: role of nearby gauged
 505 catchments for prediction at an ungauged catchment, *Hydrol. Earth Syst. Sci.*, 16(2),
 506 551–562, doi:10.5194/hess-16-551-2012.

507 Patil, S., and M. Stieglitz (2014), Modelling daily streamflow at ungauged catchments: what
 508 information is necessary?, *Hydrol. Process.*, 28(3), 1159–1169, doi:10.1002/hyp.9660.

509 Patil, S. D., P. J. Wigington, S. G. Leibowitz, E. A. Sproles, and R. L. Comeleo (2014a),
 510 How does spatial variability of climate affect catchment streamflow predictions?, *J.*
 511 *Hydrol.*, 517, 135–145, doi:10.1016/j.jhydrol.2014.05.017.

512 Patil, S. D., P. J. Wigington, S. G. Leibowitz, and R. L. Comeleo (2014b), Use of Hydrologic
 513 Landscape Classification to Diagnose Streamflow Predictability in Oregon, *JAWRA J.*
 514 *Am. Water Resour. Assoc.*, 50(3), 762–776, doi:10.1111/jawr.12143.

515 Peel, M. C., and G. Blöschl (2011), Hydrological modelling in a changing world, *Prog. Phys.*
 516 *Geogr.*, 35 (2), 249–261.

517 Post, D. A., and A. J. Jakeman (1999), Predicting the daily streamflow of ungauged
 518 catchments in S.E. Australia by regionalising the parameters of a lumped conceptual
 519 rainfall-runoff model, *Ecol. Modell.*, 123(2-3), 91–104, doi:10.1016/S0304-
 520 3800(99)00125-8.

521 Razavi, S., and B. A. Tolson (2013), An efficient framework for hydrologic model calibration
 522 on long data periods, *Water Resour. Res.*, 49(12), 8418–8431,
 523 doi:10.1002/2012WR013442.

524 Refsgaard, J. C. (1997), Parameterisation, calibration and validation of distributed
 525 hydrological models, *J. Hydrol.*, 198(1-4), 69–97, doi:10.1016/S0022-1694(96)03329-
 526 X.

527 Refsgaard, J. C., and J. Knudsen (1996), Operational Validation and Intercomparison of
 528 Different Types of Hydrological Models, *Water Resour. Res.*, 32, 2189–2202,
 529 doi:10.1029/96wr00896.

530 Refsgaard, J. C. et al. (2014), A framework for testing the ability of models to project climate
 531 change and its impacts, *Clim. Change*, 122(1-2), 271–282, doi:10.1007/s10584-013-
 532 0990-2.

533 Singh, R., T. Wagener, K. van Werkhoven, M. E. Mann, and R. Crane (2011), A trading-
 534 space-for-time approach to probabilistic continuous streamflow predictions in a

535 changing climate – accounting for changing watershed behavior, *Hydrol. Earth Syst.*
536 *Sci.*, 15(11), 3591–3603, doi:10.5194/hess-15-3591-2011.

537 Singh, R., K. van Werkhoven, and T. Wagener (2014), Hydrological impacts of climate
538 change in gauged and ungauged watersheds of the Olifants basin: a trading-space-for-
539 time approach, *Hydrol. Sci. J.*, 59(1), 29–55, doi:10.1080/02626667.2013.819431.

540 Sivapalan, M. et al. (2003), IAHS Decade on Predictions in Ungauged Basins (PUB), 2003–
541 2012: Shaping an exciting future for the hydrological sciences, *Hydrol. Sci. J.*, 48, 857–
542 880, doi:10.1623/hysj.48.6.857.51421.

543 Slack, J. R., A. Lumb, and J. M. Landwehr (1993), *Hydro-Climatic Data Network (HCDN)*
544 *Streamflow Data Set, 1874-1988*., U.S. Geological Survey, Reston, VA.

545 Vaze, J., D. A. Post, F. H. S. Chiew, J.-M. Perraud, N. R. Viney, and J. Teng (2010), Climate
546 non-stationarity – Validity of calibrated rainfall–runoff models for use in climate change
547 studies, *J. Hydrol.*, 394(3-4), 447–457, doi:10.1016/j.jhydrol.2010.09.018.

548 Wagener, T., and H. S. Wheater (2006), Parameter estimation and regionalization for
549 continuous rainfall-runoff models including uncertainty, *J. Hydrol.*, 320, 132–154,
550 doi:10.1016/j.jhydrol.2005.07.015.

551 Wagener, T., N. McIntyre, M. J. Lees, H. S. Wheater, and H. V Gupta (2003), Towards
552 reduced uncertainty in conceptual rainfall-runoff modelling: dynamic identifiability
553 analysis, *Hydrol. Process.*, 17(2), 455–476, doi:10.1002/hyp.1135.

554 Wagener, T., M. Sivapalan, P. A. Troch, B. L. McGlynn, C. J. Harman, H. V Gupta, P.
555 Kumar, P. S. C. Rao, N. B. Basu, and J. S. Wilson (2010), The future of hydrology: An
556 evolving science for a changing world, *Water Resour. Res.*, 46(5), W05301,
557 doi:10.1029/2009WR008906.

558 Wang, R., and L. Kalin (2011), Modelling effects of land use/cover changes under limited
559 data, *Ecohydrology*, 4(2), 265–276, doi:10.1002/eco.174.

560 Westra, S., M. Thyer, M. Leonard, D. Kavetski, and M. Lambert (2014), A strategy for
561 diagnosing and interpreting hydrological model nonstationarity, *Water Resour. Res.*,
562 50(6), 5090–5113, doi:10.1002/2013WR014719.

563 Xia, Y., Z.-L. Yang, C. Jackson, P. L. Stoffa, and M. K. Sen (2004), Impacts of data length
564 on optimal parameter and uncertainty estimation of a land surface model, *J. Geophys.*
565 *Res. Atmos.*, 109(D7), D07101, doi:10.1029/2003JD004419.

566 Young, A. R. (2006), Stream flow simulation within UK ungauged catchments using a daily
567 rainfall-runoff model, *J. Hydrol.*, 320, 155–172, doi:10.1016/j.jhydrol.2005.07.017.

568 Zhang, X., R. Srinivasan, K. Zhao, and M. Van Liew (2009), Evaluation of global
569 optimization algorithms for parameter calibration of a computationally intensive
570 hydrologic model, *Hydrol. Process.*, 23(3), 430–441, doi:10.1002/hyp.7152.

571 Zhang, Y., and F. H. S. Chiew (2009), Relative merits of different methods for runoff
572 predictions in ungauged catchments, *Water Resour. Res.*, 45, W07412–W07412,
573 doi:10.1029/2008WR007504.

574

575

Table 1: Comparison of the two catchment groups (from Figure 9) in terms of mean annual rainfall, annual runoff ratio and climate aridity index.

Catchment group	Median value of mean annual rainfall (P)	Median value of annual runoff ratio (Q/P)	Median value of climate aridity index (PET/P)
Group 1: Spatial or spatiotemporal transfer performs best	1110 mm	0.43	0.73
Group 2: Temporal transfer performs best	1185 mm	0.41	0.69

Figures

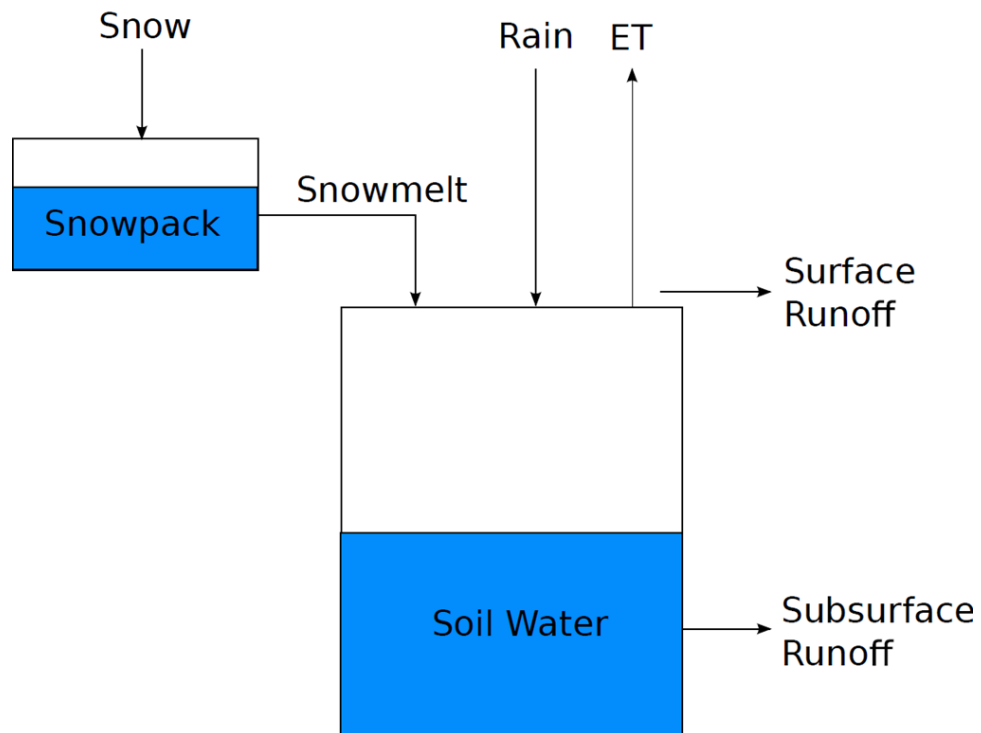


Figure 1: Overview of the EXP-HYDRO model components and fluxes (from *Patil et al.* [2014a]).

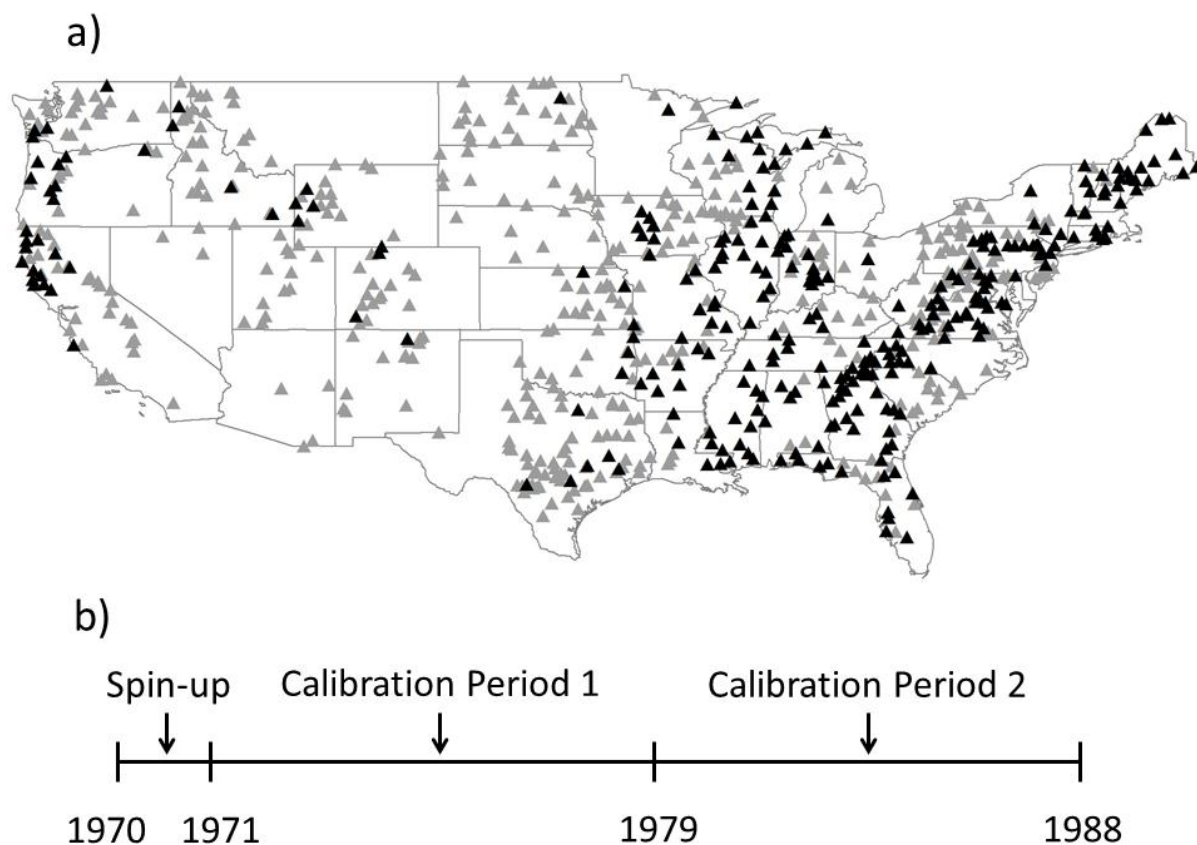


Figure 2: a) Location of all 756 catchments within the continental US where the EXP-HYDRO model is implemented; the 294 study catchments that are retained for parameter transfer experiments are shown in black triangles, and b) Schematic representation of the timeline of the calibration periods.

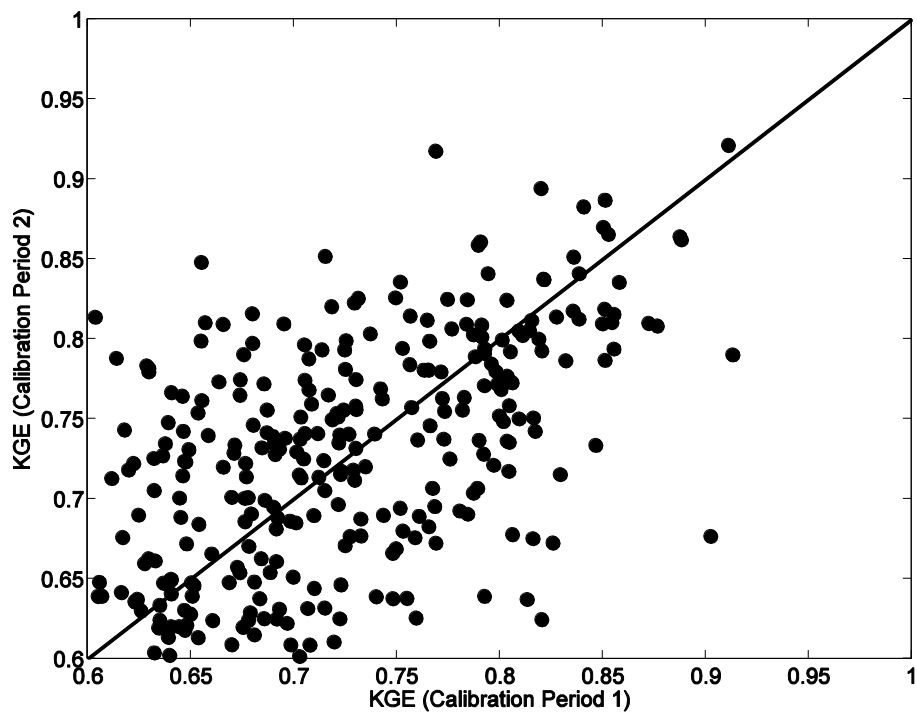


Figure 3: A 1:1 comparison of the KGE values for Calibration Periods 1 and 2.

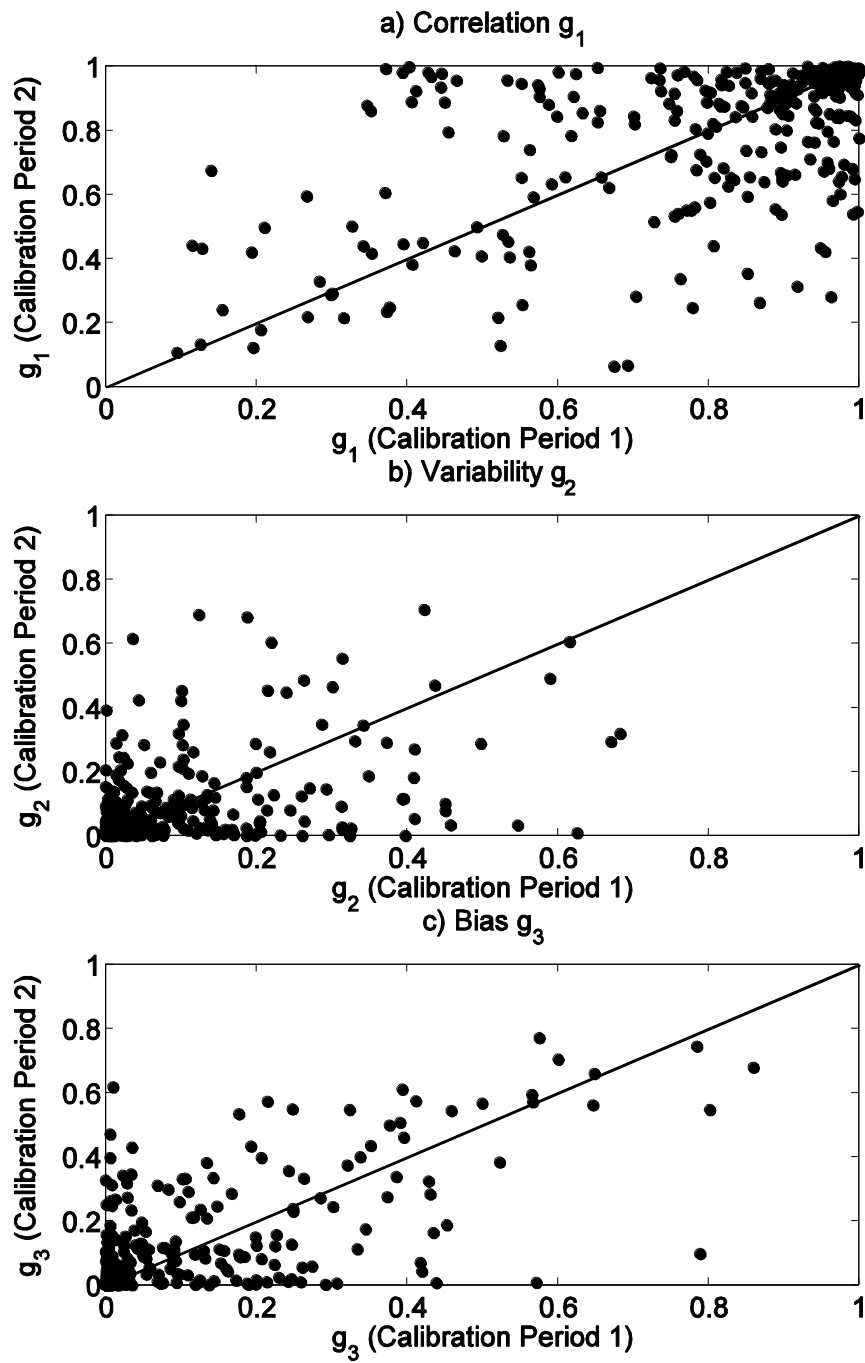


Figure 4: A 1:1 comparison of the three KGE components for Calibration Periods 1 and 2: a) Correlation g_1 , b) Variability g_2 , and c) Bias g_3 .

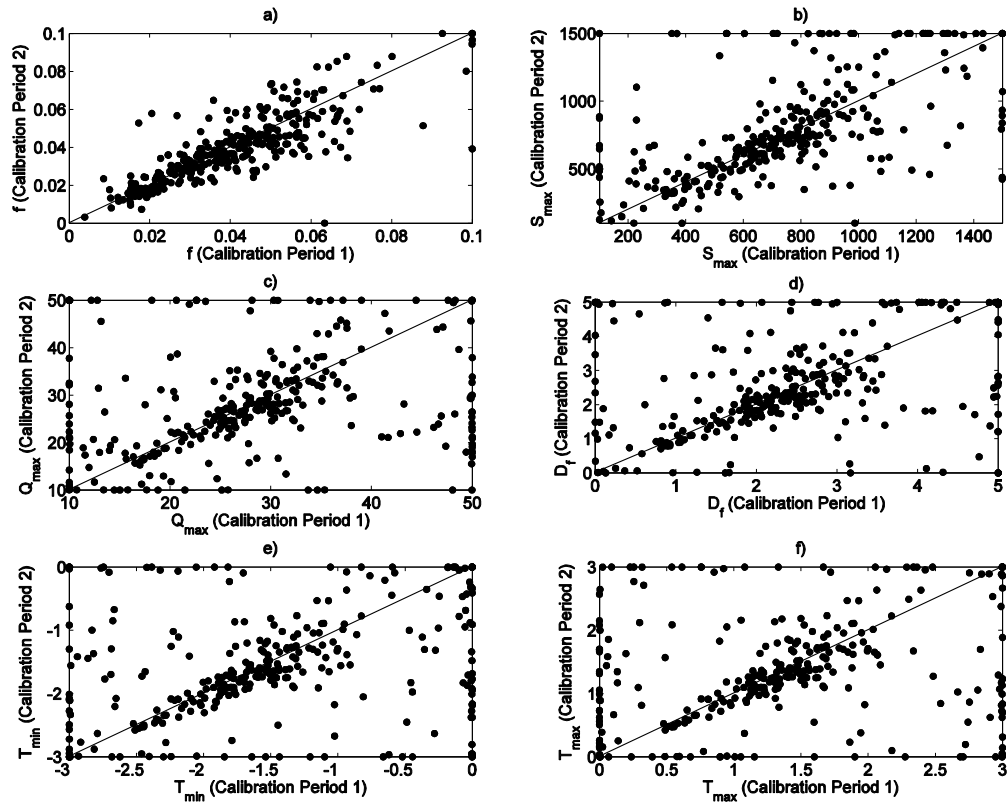


Figure 5: A 1:1 comparison of all 6 EXP-HYDRO parameter values for Calibration Periods 1 and 2.

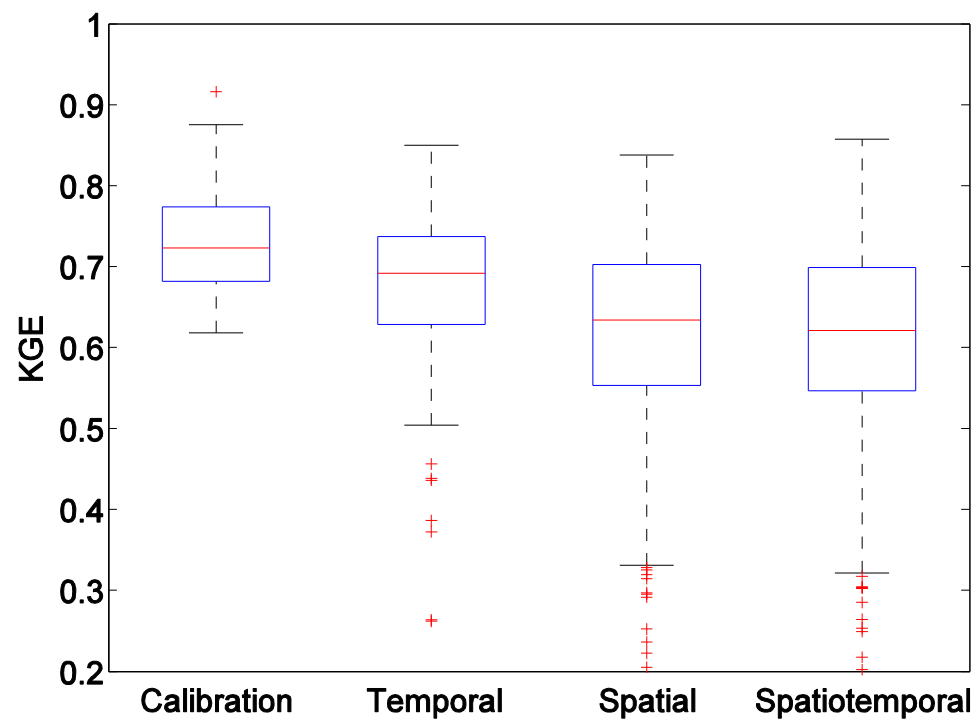


Figure 6: A box-plot comparison of the KGE values for calibration and the three parameter transfer scenarios.

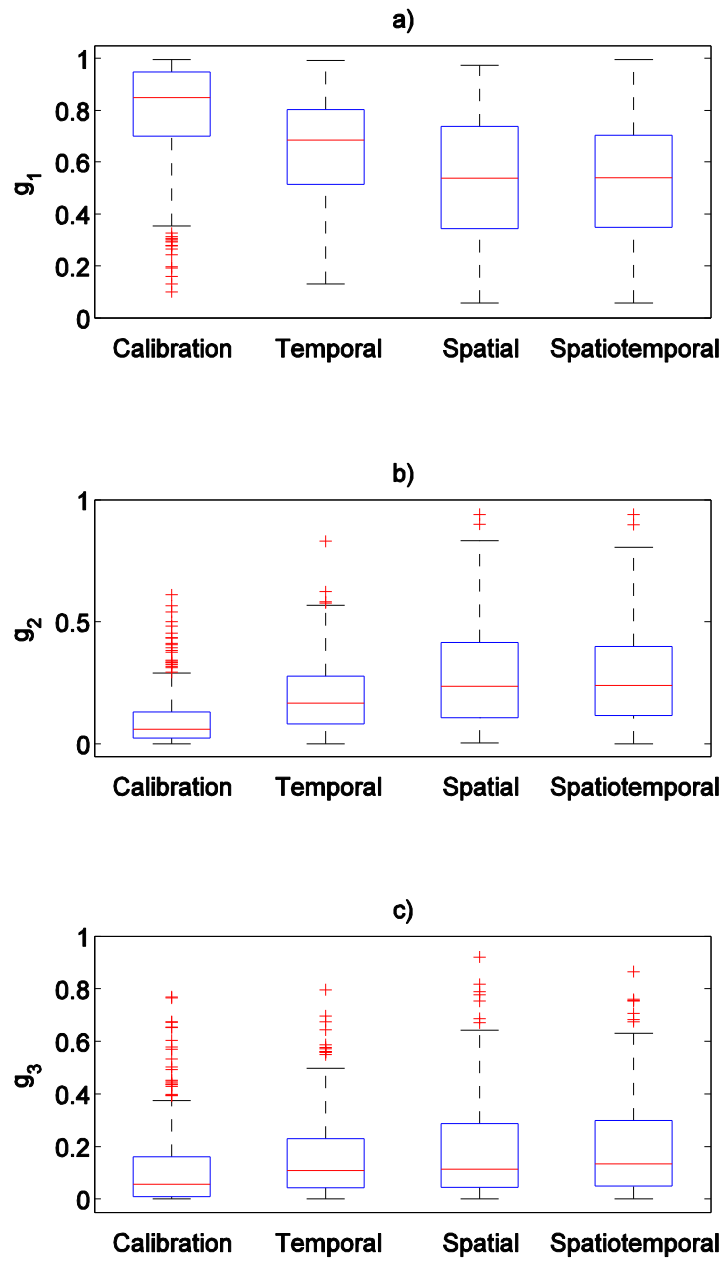


Figure 7: A box-plot comparison of the three KGE components for calibration and the three parameter transfer scenarios.

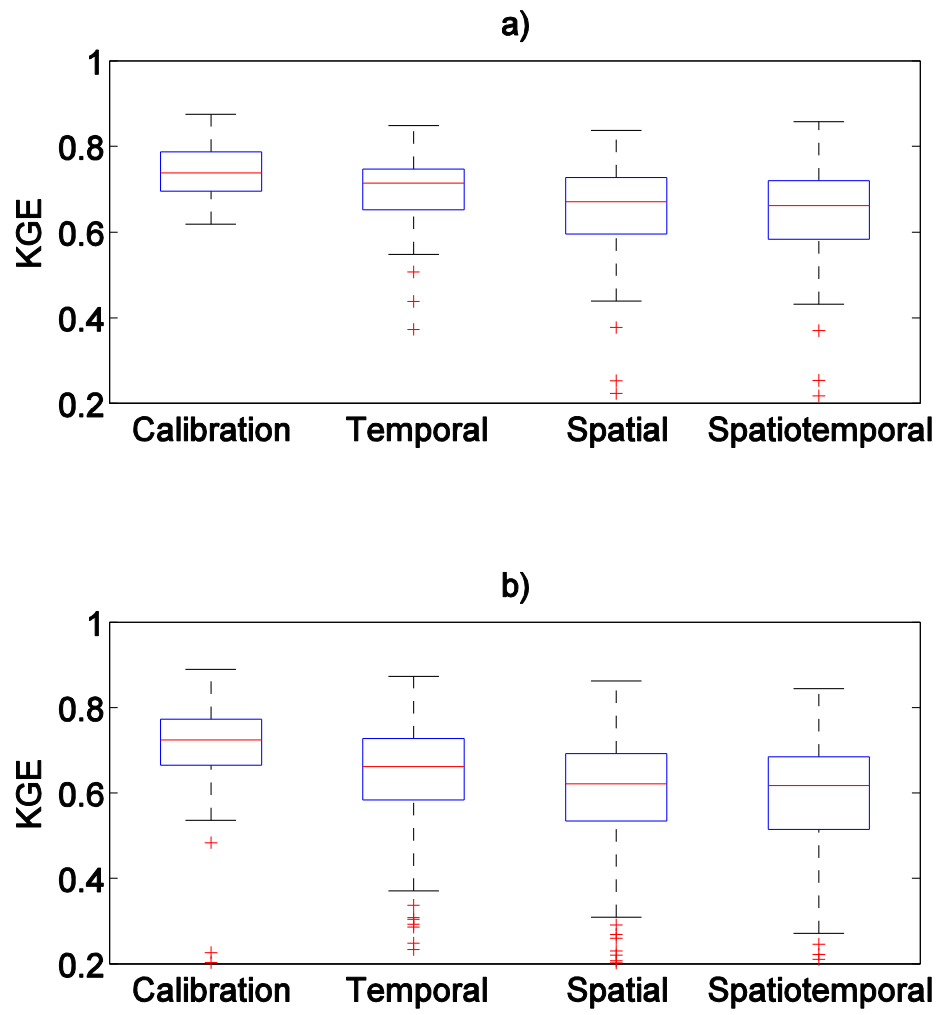


Figure 8: A box-plot comparison of the KGE values for calibration and the three parameter transfer scenarios, shown separately for a) Special Condition 1, and b) Special Condition 2.

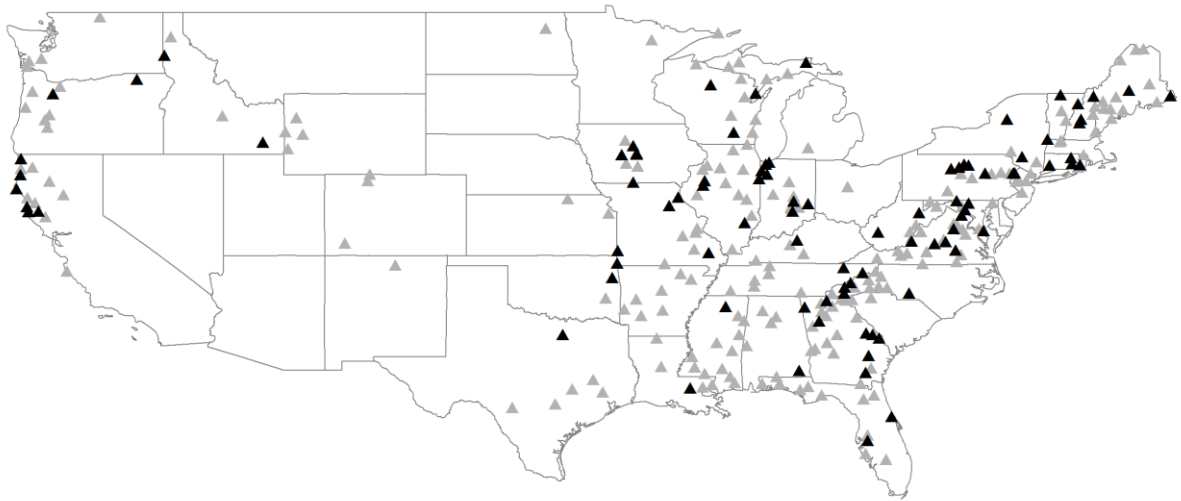


Figure 9: Location of the catchments where either the spatial or spatiotemporal parameter transfer scheme performs best (Black triangles). Catchments where the temporal parameter transfer scheme performs best are shown as grey triangles.